Polymer Testing 150 (2025) 108925

Contents lists available at ScienceDirect

Polymer Testing

journal homepage: www.elsevier.com/locate/polytest

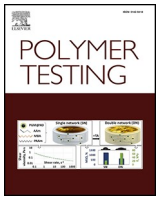

Mid- and near-infrared spectroscopies for quantitative tracking of isocyanate content: Streamlined development of monitoring tools for reactive extrusion synthesis of specialty polyurethanes

Aleksandra M. Fage [a,*], Christian A. Backhaus [a], Wolfgang Becker [a], Günter Lorenz [b], Anita Lorenz [b], Karsten Rebner [b], Frank Henning [a,c]

[a] Fraunhofer Institute for Chemical Technology, Joseph-von-Fraunhofer-Strasse 7, Pfinztal, 76327, Germany
[b] Reutlingen University, Faculty of Life Sciences, Alteburgstrasse 150, 72762, Reutlingen, Germany
[c] Karlsruhe Institute of Technology, Rintheimer-Querallee 2, 76131, Karlsruhe, Germany

ARTICLE INFO

Keywords:
Polyurethane
Isocyanate quantification
Near-infrared spectroscopy
Mid-infrared spectroscopy
Partial Least Squares regression model
Process monitoring

ABSTRACT

Robust in-situ monitoring can expedite the development and tuning of reactive extrusion (REX) processes, especially for the synthesis of polymers requiring insight into the reaction course, such as specialty polyurethanes (PUs). In order to advance the feasibility of such analysis, our research concentrated on a spectroscopic protocol that combines at-line mid-infrared (MIR) and on-line near-infrared (NIR) measurements in a laboratory extruder, assessing both their qualitative and quantitative capabilities. To mimic the depletion of the reactive species during polymerisation, a series of premixes were formulated and characterised under non-reactive conditions using a benchmark pair of a polyol and a diisocyanate. By this means, we identified suitable spectral features for quantifying isocyanate content via multivariate regression models. This approach achieved good calibration metrics for both MIR and NIR models and enabled a robust assessment of their predictive performance through cross-validation, using only a moderate number of spectral datasets. Our work is therefore the first step towards establishing a method for in-process NIR analysis with streamlined at-line MIR verification. It provides a shortcut for designing monitored REX syntheses of PUs and other material systems amenable to quantitative calibration based on spectroscopic data from raw reagents.

1. Introduction

Reactive extrusion (REX) is increasingly favoured in the production of specialty polymers and additives because of its efficiency and adaptability as a process that enables both polymerisation and modification within a continuous, solvent-free synthesis [1–5]. Its ability to tailor the molecular architecture and integrate functional groups allows the creation of materials with highly specific properties. Consequently, overcoming the constraints of conventional batch synthesis by transfer into REX manufacturing is a key strategy for cases where effective mixing of viscous reagent streams not only determines the product quality, but also enhances reaction kinetics. However, the polymerisation of monomeric components via REX is inherently complex, involving chemical and physical transitions in the melt that are interconnected with the processing conditions [1,6]. Monitoring of these aspects is particularly relevant in the production of thermoplastic polyurethanes (PUs), where the structure, and consequently the performance, of the final product can be significantly altered by the chemical pathways of the synthesis and the technical precision in the process design [7–10]. As PUs are obtained through step-growth polyaddition between polyols and polyisocyanates, the system is highly sensitive to reagent stoichiometry, temperature conditions, and excess water residues [11,12]. Therefore, without effectively identifying the phenomena in the PU reaction, the REX process can be operated as a “black box”, which is suboptimal in terms of overall efficiency [13–17]. Implementing analyses that ensure comprehensive insights into the material system is therefore crucial not only for research and development but also for production control requiring rapid and precise feedback.

Among the sensing technologies common in the extrusion processing of polymers — including rheometric, ultrasonic or spectroscopic — the latter stands out for its ability to provide detailed information on both material characteristics and process stability [13,14,18]. While the

* Corresponding author.
E-mail address: aleksandra.fage@ict.fraunhofer.de (A.M. Fage).

https://doi.org/10.1016/j.polymertesting.2025.108925
Received 14 April 2025; Received in revised form 25 June 2025; Accepted 10 July 2025
Available online 10 July 2025

conventional at-line spectroscopic measurements serve as complementary verification tools, the probes implemented in-line within the extruder or through an on-line configuration within adjacent equipment are designed for real-time monitoring [13]. For example, ultraviolet–visible and fluorescence spectroscopies are frequently applied to assess concentration of additives, measure residence time distributions and detect degradation in polymer melts [13,19]. Vibrational spectroscopies, such as mid-infrared (MIR) [15,20–22], near-infrared (NIR) [16,23–27], and Raman [13,15,28], are effective for analysing the molecular architecture of polymeric materials, making them particularly useful for evaluating chemical transitions during REX.

Appropriate selection of the vibrational spectroscopic techniques not only provides insight into the qualitative aspects but also enables the quantification of detected species through a linear relationship with spectral absorbance, following the Beer-Lambert law [16,29]. Their applicability to a material system depends on the spectral range corresponding to the vibrations of that system, and on the complexity of the spectral data [15,18,25]. Changes in the content of functional groups, which appear as sufficiently defined or isolated bands, can be correlated with the progress of the reaction using straightforward evaluation involving linear regression [16,24,30]. In contrast, spectral regions with bands that overlap or are difficult to assign require advanced chemometric methods to extract meaningful information [24,25,28,31,32]. Such methods rely on multivariate data analysis, which interprets and evaluates complex datasets. For instance, intricate relationships between spectral data and material properties can be quantified by models calculated using Partial Least Squares (PLS) regression algorithms [24,28,32–34]. These techniques effectively address noise in collinear data, as they identify latent variables, i.e. factors, that explain the covariance between predictors (e.g., spectral data) and response variables (e.g., reagent concentration). In this approach, developing a quantification model requires training on spectra from materials with known formulations, ensuring that the calibration is based on representative data. Consequently, robustness of the model relies on capturing relevant information from wavenumber regions corresponding to specific chemical functionalities [25], while maximising the signal-to noise ratio by tailored pretreatment [25,28,34] of the original data.

The diagnostic region in MIR spectroscopy is highly effective for identifying fundamental vibrations in PU materials, enabling precise distinction between bands characteristic of the monomers [15,29,30,35]. The depletion of reactive species can therefore be evaluated through changes in peak areas corresponding to their functional groups, following adequate normalization of the spectra on a reference band, which is inert during the reaction. As shown by Madra et al. [30], MIR analysis applied at-line during the batch synthesis of oil-based PUs tracked the conversion by relating the absorption band of the isocyanate group to a cluster of aliphatic absorption bands in the diagnostic area, used as an internal standard. Their approach included a calibration step using material premixes with known formulations to generate a standard curve for absolute quantification, which was additionally validated through back-titration measurements of the isocyanate content. Nevertheless, despite its high detection sensitivity, MIR spectroscopy is rarely used for in-situ analysis in extrusion due to its shallow penetration depth in polymer melts, typically limited to surface measurements of a few micrometres [13,20,21]. Additionally, advanced MIR probes are expensive, have limited durability, and require controlled environments for optimal performance [13,20,22].

Considering the practical aspects of process analytics, NIR spectroscopy is a frequent choice for in-situ monitoring in reactive PU manufacturing, offering effective characterisation up to a few millimetres into the melt, with commercially available probes designed for demanding conditions [18,36]. However, as the absorptions in the NIR region appear as broad and overlapping bands, originating from overtones and combinations of fundamental vibrations, they are less distinctive than those in the MIR range and require more advanced pretreatment [31,32]. Moreover, the NIR technique is inherently sensitive to physical phenomena that affect the light scattering in the measured matrix — such as changes in temperature influencing the morphology or homogeneity of the material — which are embedded in the spectra alongside the chemical information [18,25,32]. As a result, in-situ NIR monitoring requires a highly controlled and reproducible processing environment [13], and developing a robust protocol depends on thorough investigation of the system supported by confirmatory off-line characterisation [15,23,27,34]. For example, Dethomas et al. [23] focused on directly evaluating the conversion during batch PU production on a pilot scale by identifying relevant features corresponding to isocyanate species in second-derivative NIR spectra. To establish a quantitative correlation, real-time NIR measurements conducted in the reactor were linked to the decreasing isocyanate concentration determined through back-titration, following time-sensitive sampling of representative specimens from the reactive mixture. The multivariate regression model achieved a standard error of calibration of ca. 0.25 %, closely aligning with the reference method and accurately estimating isocyanate concentrations when applied to a production case under conditions identical to the calibration.

Overall, literature reports demonstrate that sufficient insight into spectral data, verified through complementary quantitative measurement, is crucial for accurately tracking progress during reactive polymer processing. Provided that accurate reference analyses of exemplary material fractions are technically feasible, spectroscopic monitoring protocols can be conceptualised and adapted directly within an industrial setup and are therefore often kept confidential [13,23]. However, this remains a significant bottleneck in the development of monitoring technologies for new, non-optimized REX approaches, which rely on fast reaction kinetics and typically do not allow facile sampling of material at different conversion stages along the extruder-reactor. The challenge is exacerbated by modular use of REX processes that offer high flexibility in both process design and the chemical composition of products. Thus, expediting the application of in-process spectroscopy requires drop-in research strategies to advance effective transfer from low technology readiness levels to scalable production lines. It involves straightforward experimental methods for in-situ investigation, supported by streamlined off-line verification, both of which can be adapted to a variety of material formulations.

Our work focused on combining NIR and MIR spectroscopy protocols for both qualitative and quantitative evaluation of material systems used in synthesis of specialty PUs. The concept was to create a toolset for robust in-situ monitoring and rapid off-line control that provides comprehensive insight into the material, with a future aim of implementing it during early-stage development of a REX production process. For this purpose, we utilised NIR analysis conducted on-line in a capillary bypass of a laboratory-scale twin-screw extruder, enabling a reproducible setting for the in-situ NIR measurements and resembling a controlled melt-processing environment. Simultaneous at-line investigation using the MIR technique aimed to replace titration or thermal methods, significantly reducing the effort involved in reference analyses [15,23,29,30], which are routinely required in production, e.g. verifying stability of in-process monitoring protocols against probe wear. As a case study demonstrating the approach, we selected a reagent system suitable for the synthesis of hydrophobically modified ethoxylated urethanes (HEURs, Scheme 2), which are commercially used as waterborne rheology modifiers. Typical HEURs are linear telechelic polymers with a hydrophilic backbone of around 20–35 kg mol^{-1}, obtained from high-molar-mass poly(ethylene glycol) (PEG) and cyclo-/aliphatic diisocyanate, which is end-capped by a short hydrophobic alcohol [37]. Such HEURs demand stringent architectural control that is inherently challenging to achieve in conventional batch production but could be effectively addressed through REX [9,12,37,38]. As our approach (Scheme 2) precedes the development of the REX synthesis method, spectroscopic characterisation was performed using non-reactive premixes of a selected polyol and diisocyanate, with the aim of mimicking the depletion of isocyanate species during polymerisation by

appropriately varying the formulation. This enabled acquisition of a sufficiently broad spectral dataset across a wide range of isocyanate concentrations for building a quantitative calibration model, while also circumventing typical limitations in sampling low-conversion states of fast-reacting systems. Tailored pretreatment of both MIR and NIR spectra revealed bands relevant for diagnostic analysis of the system and enabled the isolation of regions strongly correlated with changes in material concentration. The obtained datasets were used to calculate PLS multivariate regression models quantifying the diisocyanate component based on both spectroscopic techniques, allowing a comparison of their performance. In this framework, we therefore demonstrate a streamlined strategy for developing a spectroscopic monitoring tool that can support preliminary investigation of a REX process, allowing convenient at-line MIR testing to corroborate the in-situ NIR analyses.

2. Experimental

2.1. Materials

Poly(ethylene glycol) Polyglykol 8000 S (PEG 8k, approx. $\overline{M}_n$ = 8000 g mol^{-1}, mp = 55–60 °C, material data provided by the supplier) was donated by Clariant AG. Dicyclohexylmethane-4,4′-diisocyanate Desmodur® W (HMDI, isocyanate group (NCO) content of 31.81 ± 0.04 wt% determined according to DIN EN 1242, Table S1) from Covestro AG was donated by CSC JÄKLECHEMIE GmbH. The materials were handled and stored under argon.

2.2. Setup for spectroscopic measurements

Mid-infrared (MIR) spectroscopic analyses were carried out at-line using a Bruker ALPHA II Fourier-transform MIR (FT-MIR) spectrometer equipped with a platinum HP Diamond attenuated total reflectance unit and operated with OPUS Bruker software. The spectra were recorded in a range between 4000 and 400 cm^{-1} with a spectral resolution of 4 cm^{-1} and 16 scans per spectrum.

Near-infrared (NIR) spectroscopic measurements were performed in both at-line and on-line mode using a Bruker Matrix-F Duplex Fourier-transform NIR (FT-NIR) spectrometer, operated with OPUS Bruker software. The setup for on-line analysis included a Sentronic optical probe equipped with a fibre bundle and a sapphire glass window. At-line characterization was carried out using a non-contact Bruker NIR sensor head Q412/A with two built-in tungsten light sources and coupled with a fibre-optic cable. The spectra were collected in a transflection mode in a range between 12000 and 4000 cm^{-1}, with a spectral resolution of 16 cm^{-1} at 32 scans per spectrum for the at-line analysis, and a resolution of 4 cm^{-1} at 8 scans per spectrum for the on-line recording. The reference intensity was measured using a white Spectralon reflectance standard.

2.3. Setup for extrusion process with spectroscopic measurements

Extrusion experiments were carried out in a Thermo Scientific HAAKE MiniLab II twin-screw extruder (laboratory scale, conical co-rotating screws with conveying design; length 109.5 mm, diameter tapering from 14 mm to 5 mm). Process parameters were controlled using HAAKE PolySoft OS software.

The extruder has an integrated backflow channel, connecting the outlet of the screw channel, located before the die, with a section positioned downstream of the feeding port (Scheme 1). The direction of the flow is set with a bypass valve, which allows either full recirculation of the melt within a controlled dwell time or discharge through the die.

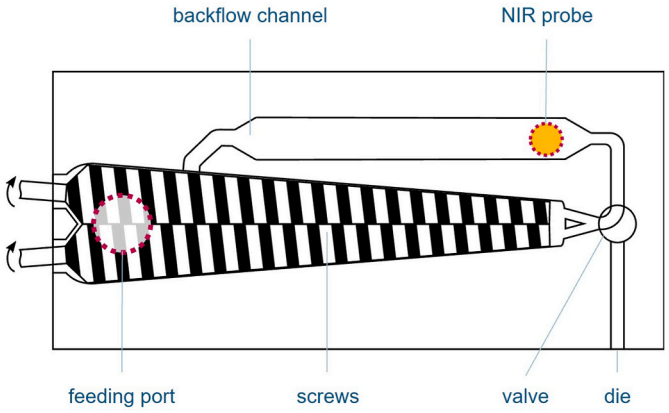

Scheme 1. Cross-section of the laboratory twin-screw extruder with the NIR probe installed in the backflow channel (adapted from [56]).

Adequate filling of the extruder requires between 6.8 and 7.4 g of the polymer per charge. The backflow channel is designed as a slit capillary with a height of 1.5 mm and includes ports for inserting sensors allowing on-line measurements during material circulation. In the applied extruder setup, the NIR optical probe was installed in the upper inlet port of the capillary.

2.4. Spectroscopic characterisation of model premixes and raw components

Model premixes, containing PEG 8k and HMDI at concentrations between 0.06 and 5.22 wt%, and a specimen of pure PEG 8k were characterised according to a protocol combining on-line NIR measurements in the extruder and simultaneous at-line MIR testing (Table S2). In preparation of each formulation, approx. 30 g of PEG 8k was placed in a 100 ml double-neck round-bottom flask, which was dried and weighed prior to the experiment. The material was melted and dehydrated in a vacuum oven at 80 °C and 10 mbar for a minimum of 12 h, applying nitrogen flushing every 1 h. Afterwards, the flask was septum-sealed and weighed to determine the precise amount of dried PEG 8k (water content of ca. 0.04 ± 0.01 wt% determined by Karl Fisher titration as described in the Supplementary Information, Table S3), and subsequently secured in a heating mantle, set to maintain the melt temperature at approx. 75 ± 2 °C. Next, the main flask neck was fitted with a dissolver-type mechanical stirrer and an argon line. The required amount of HMDI was then injected through the septum-sealed side neck using a syringe and the components were mixed at 1000 rpm for ca. 90 s. The obtained premix was directly used for the spectroscopic characterisation.

For the at-line MIR analyses ca. 0.2 g of the melt was taken from the flask using a spatula and immediately placed on the module of the FT-MIR spectrometer. Each specimen was measured once, allowing for collection of 2–3 spectra per formulation within max. 5 min after its preparation.

In parallel to the MIR testing, ca. 7 g of the obtained premix was drawn from the flask using a preheated syringe and dosed into the extruder set at 70 ± 1 °C and 100 rpm for the on-line NIR analyses. Before the experiments, the extruder was switched to the circulation mode and flushed with argon through the feed port to maintain an inert atmosphere. The flow of argon was kept during the entire experimental procedure. The on-line NIR measurements began with the circulation of the premix in the extruder and were carried out continuously for ca. 2 min, until 10 spectra were collected (measuring time of approx. 12 s per

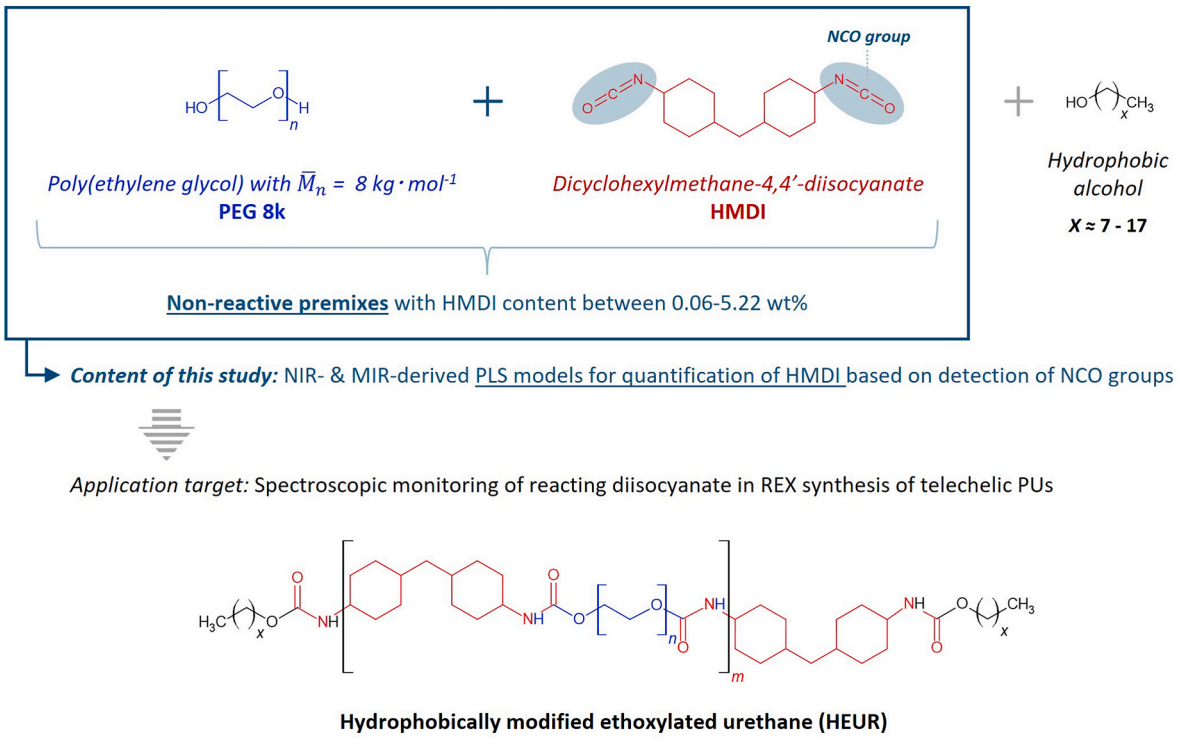

Scheme 2. Approach for developing spectroscopic calibration models to quantify content of diisocyanate in reagent mixtures, mimicking the synthesis of specialty PUs, using on-line NIR and at-line MIR analysis.

spectrum). The melt ejected from the extruder immediately after completing the NIR recording was additionally tested using at-line MIR spectroscopy to verify the stability of the material formulation and the absence of chemical changes due to the processing step.

Pristine HMDI and PEG 8k (dried and molten) were additionally characterized using both MIR and NIR techniques in at-line mode.

2.5. Preprocessing of spectroscopic data

Prior to analysis, all collected spectra were pretreated with normalization and differentiation steps to enhance their comparability and to reduce baseline effects or noise. The appropriate preprocessing parameters for the MIR and NIR spectra of the model premixes were selected based on a systematic assessment, as detailed in the Supplementary Information (Table S4–6, Fig. S1–3):

- *At-line MIR spectra:* (1) Area normalization was performed using the absorbance region 3050–2550 cm^{-1} (which contains only signals from inert aliphatic CH groups, Fig. 3), and (2) a first derivative was calculated using a Savitzky–Golay filter (second-order polynomial, 11-point window, symmetric kernel) to remove any remaining baseline offset.
- *On-line NIR spectra:* (1) Standard Normal Variate (SNV) normalization was applied to correct multiplicative scattering effects and intensity variations, (2) Savitzky–Golay smoothing (second-order polynomial, 31-point window) was used to reduce high-frequency noise, and (3) a second derivative (Savitzky–Golay, second-order polynomial, 41-point window, symmetric kernel) was calculated to eliminate baseline drift and resolve overlapping bands.
- *At-line NIR spectra:* (1) SNV normalization followed by (2) a second derivative (Savitzky–Golay, second-order polynomial, 15-point window, symmetric kernel) was sufficient to correct the baseline and supress residual noise.

The MIR spectra were normalized with OPUS Bruker software. All pretreatment steps of the NIR data and further MIR processing were performed using Solo Eigenvector Research Inc. 9.5.0 software.

2.6. Calculation of Partial Least Squares (PLS) regression for spectroscopic calibration models

The spectroscopic data from the non-reactive premixes of PEG 8k and HMDI, including a sample of pristine PEG 8k, were used to develop PLS models for quantifying the content of free HMDI in the studied material system. To calculate the PLS regression, the known HMDI concentration in the premixes (Table S3) was set as the response variable and the fully pretreated spectra of the premixes were used as the predictor dataset. The input data were restricted to spectral regions that contained the absorption bands of the NCO groups in HMDI: 2330–2200 cm^{-1} for MIR (corresponding to the NCO stretching vibrations, Fig. 3) and 5225–5050 cm^{-1} for NIR (corresponding to the NCO combination vibrations, Fig. 4).

The PLS models were generated using mean-centring and a Simplified PLS algorithm, based on 60 MIR spectra from 16 premixes (3–4 spectra per premix) and 130 NIR spectra from 13 premixes (10 spectra per premix), respectively (Table S3). Due to the grouped nature of the MIR and NIR data, where each premix is represented by multiple spectra collected under nearly identical conditions, the models were evaluated using a contiguous block cross-validation method (spectra from each premix were grouped and one group at a time was left out in rotation for computation), as described in the Supplementary Information. The applied validation strategy was additionally benchmarked against other techniques principally suited to the structure of the spectroscopic data used (Table S7–8). In both MIR and NIR models, the number of latent factors in the PLS model was chosen based on cross-validation metrics to maximize explained variance while maintaining sufficiently low model complexity. The quality of the resulting models was assessed according to the obtained coefficient of determination (R^2) and the root mean square error of calibration (RMSEC) and cross-validation (RMSECV), as summarized in Table 2. All calculations performed during the modelling steps were carried out using Solo Eigenvector Research Inc. software.

3. Results

The combination of on-line NIR and at-line MIR analysis provided insight into an exemplary HEUR reagent system and enabled the correlation of spectral information with the content of isocyanate species in the material, needed for generating PLS quantification models (Scheme 2). In this setting, the superior diagnostic capability of MIR spectroscopy supported the evaluation of data obtained from NIR analysis and its application as an in-situ monitoring tool. The investigation was carried out using non-reactive premixes of poly(ethylene glycol) with a molar mass of 8 kg mol^{-1} (PEG 8k) and dicyclohexylmethane-4,4′-diisocyanate (HMDI), suitable for building the core of a HEUR molecule. To obtain a calibration curve reflecting the decreasing content of isocyanate groups (NCO) throughout the complete course of HEUR synthesis, the concentration of HMDI in the premixes was varied between 5.22 and 0.06 wt%, additionally including pure PEG 8k (Table S2). The formulations with HMDI concentrations above 3 wt% were set to match the theoretical stoichiometry required to form chain lengths typical of a HEUR backbone, following the Carothers equation [39,40]. In the concentration range below 0.5 wt%, the ratios between the components were varied in smaller intervals to account for the decreasing detection sensitivity of the spectroscopic techniques.

The premixes, prepared in small batches, were simultaneously analysed on-line via NIR in a laboratory extruder at 70 ± 1 °C (Scheme 1) and at-line with MIR technique at room temperature. The controlled processing conditions in the extruder provided a reproducible environment for the NIR measurements, while the experimental protocol was designed to suppress the reactions of HMDI, ensuring that its structure remained intact during the analyses. To inhibit the polymerisation, the premixes were handled at mild temperatures (<80 °C) for a limited time (<5 min) after the components were combined [39,40]. Moreover, a supporting Karl Fischer titration study showed that the water content in the dried PEG 8k remained within a stable range of 0.04 ± 0.01 wt% throughout the entire procedure (Table S3), aligning with typical industrial limit for PU manufacture [40] and preventing detectable consumption of NCO groups by reaction with water [11,41]. Detailed qualitative investigation of the obtained premixes ensured that the added material formulations could be accurately correlated with the features detected in both NIR and MIR spectra of the individual reagents, establishing a clear link for quantitative analysis.

3.1. Spectroscopic characterisation of model premixes

To unify the absorbance intensity between the individual MIR measurements of the premixes, all raw spectra (Fig. 1a) were normalized on the peak area between 3050 and 2550 cm^{-1}, corresponding to the vibrations of CH groups in the backbone of both components [42]. For PEG 8k, the MIR normalization region contains multiple overlapping bands (Fig. 2a). The medium-intensity band at 2880 cm^{-1} and a small shoulder at 2945 cm^{-1} correspond to the symmetric and asymmetric stretching of aliphatic CH_2 groups, respectively [42–44]. Further absorption bands between 2860 and 2700 cm^{-1} can be assigned to combinations of fundamental CH vibrations from the fingerprint region [42–44]. The cycloaliphatic and aliphatic CH_2 groups in HMDI (Fig. 2a) show two sharp bands at approx. 2930 cm^{-1} and 2856 cm^{-1}, due to the asymmetric and symmetric stretching, respectively, overlapping with a shoulder around 2900 cm^{-1} related to vibrations of tertiary cycloaliphatic CH groups [42]. The selected normalization region is well-separated from other characteristic bands and remains inert during the polymerisation reaction. Therefore, the normalization step should be similarly effective when applied to spectra of a reactive mixture and should respond to the presence of additional reagents depending on their aliphatic structure [29,30]. The corrected spectra of the premixes showed good reproducibility across individual samplings (Fig. 3a, Figure S4-19), distinguishing the contributions of the aliphatic structures of PEG 8k and HMDI.

The unique spectral features of PEG 8k and HMDI, detected in the normalized MIR spectra of the model premixes, were verified based on the separate analysis of the pristine reagents presented in Fig. 2a. The characteristic bands of the components are listed in Table 1 and the relevant areas in the premixes are labelled in Fig. 3a. Due to the high molar mass of PEG 8k, the stretching vibrations of its terminal hydroxyl groups (OH) produce a minor band around 3485 cm^{-1}, which is not evident in the spectra of the premixes, while the asymmetric stretching of ether bonds (C–O) in the repeating unit appears as a very strong absorption at ca. 1096 cm^{-1} [43,44]. The spectrum of HMDI shows two bands, arising from the fundamental vibrations of NCO groups, which positively correlate with its concentration in the premixes. The well-defined band visible at 2262 cm^{-1} corresponds to the asymmetric stretching of NCO groups and the smaller band at 577 cm^{-1} is ascribed to their bending modes [42,45]. Additional vibrations characteristic for pristine HMDI are not distinguished in the premixes due to their low absorption. The broad band at approx. 3680 cm^{-1} comes from the first overtone of the asymmetric NCO stretching [46], which also shows a characteristic shoulder [42] around 2110 cm^{-1}. The minor peak visible at 1762 cm^{-1} can be associated with the stretching of carbonyl group (C=O) in uretdione rings [47–50] from trace amounts of dimerized HMDI. The remaining vibrations representative for the individual

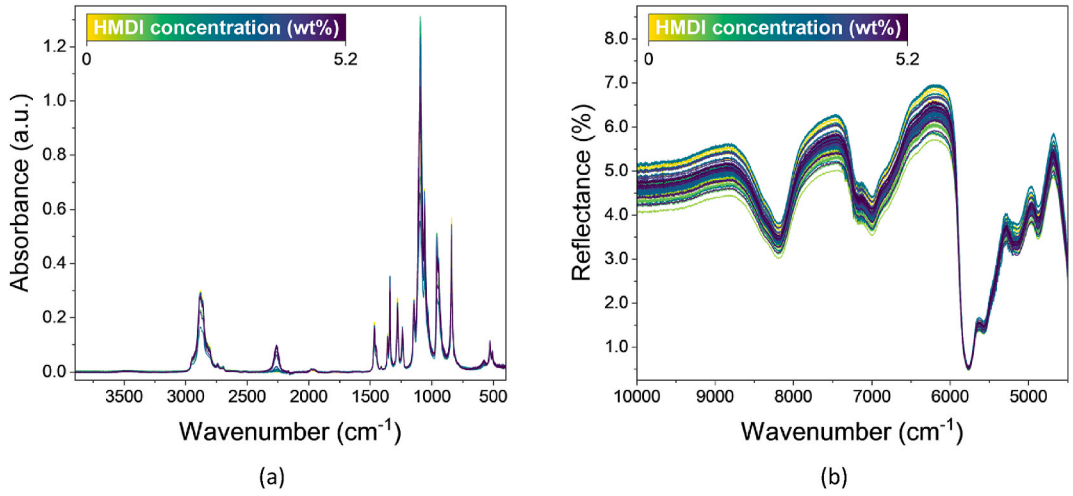

Fig. 1. Raw spectra of model premixes containing PEG 8k and HMDI at varied concentrations: (a) At-line MIR analysis; (b) On-line NIR analysis in a bypass capillary of a laboratory extruder.

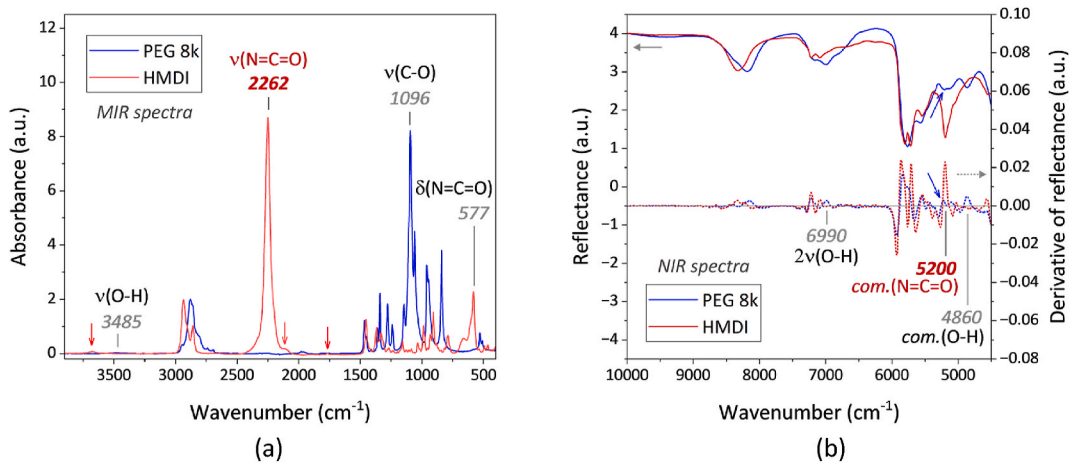

Fig. 2. Spectral data of PEG 8k and HMDI with highlighted characteristic bands (*ν*: stretching modes, δ: bending modes, com.: combination vibrations): (a) MIR spectra; (b) NIR spectra.

components overlap with aliphatic absorption frequencies in the fingerprint region [42]. Moreover, the stretching of the OH groups from water, appearing at around 3300 cm^{-1}, was not detected, as its residual content approached the sensitivity threshold of the MIR technique for this type of vibrations [42].

The absence of chemical changes in the reagent system was additionally verified by MIR for each premix sampled from the batch flask and for material ejected from the extruder immediately after the on-line NIR measurement. None of the spectra showed vibrations in the range between 1750 and 1500 cm^{-1}, indicating that neither urethane species nor urea or amine by-products were formed via reactions of the NCO group under the studied conditions [11,12,45]. This confirmed that the molecular structure and composition of the premixes remained unchanged during both analytical protocols, providing reliable spectral data for quantitative correlation.

The NIR spectra recorded on-line for the model premixes and at-line for the respective reagents showed a good signal-to-noise ratio, while the scattering effects caused significant variation in the spectral features, requiring correction prior to qualitative analysis. To account for the fundamental differences between the NIR and MIR techniques, particularly the sensitivity of NIR to the physical aspects of the measurement, the pretreatment method and its parameters were tailored accordingly. Major fluctuations in intensity and baseline offset visible in the raw NIR spectra (Fig. 1b) were initially reduced through Standard Normal Variate normalization. The subsequent smoothing by Savitzky-Golay algorithm minimized noise and enhanced clarity of the spectral features (Fig. 4a). Finally, calculating a second-order Savitzky-Golay derivative eliminated the baseline drift and improved the resolution of closely spaced and overlapping bands (Fig. 4b). The second-derivative NIR spectra showed positive bands flanked by negative side-lobes, with maxima occurring at the same wavenumbers as the characteristic absorptions in the zero-order spectrum, enabling their assignment.

The characteristic absorptions of the reagents, identified in Fig. 2b, are listed in Table 1 and indicated in the NIR spectra of the premixes, shown in Fig. 4a and b. For all components, the upper NIR region contains bands from the second overtone of CH stretching vibrations, appearing between 8700 and 8000 cm^{-1}, and from ternary CH combination vibrations between 7400 and 6600 cm^{-1} [32,51]. Additionally, a very strong absorption due to the first stretching overtone of CH is observed around 6200–5500 cm^{-1} [32,51]. The differences in aliphatic structure between PEG 8k and HMDI are reflected in the spectral features of the premixes, showing minor variations in the derivative spectra at approx. 7200 cm^{-1} and 5750 cm^{-1}.

The area in the premixes corresponding to the CH combination in the upper NIR range overlaps with the first stretching overtone of OH groups, located for PEG 8k at ca. 6990 cm^{-1}, which can be assigned to non-hydrogen-bonded species [52,54]. The series of minor bands at approx. 6790, 6670 and 6410 cm^{-1} could predominantly arise from OH groups contributing to hydrogen-bonding interactions within the matrix [54]. Due to their decreasing intensity, higher OH overtones, typically found above 10000 cm^{-1}, are not distinguished in the spectra of the premixes [32,42]. The complex spectral patterns visible in the lower NIR region between ca. 5600–4500 cm^{-1} occur due to CH combination modes, which could be coupling with OH vibrations in PEG 8k around 4860 cm^{-1} [52,54]. In contrast to MIR, differences in absorbance of the major OH bands are detectable in the NIR spectra depending on the formulation. Furthermore, the bands from aliphatic species in the lower NIR range overlap with NCO combination vibrations, which in pure HMDI produce a strong band around 5200 cm^{-1} [53]. Several wavenumber fragments adjacent to the NCO band in the NIR spectra of the premixes show a trend correlating with the ratio between PEG 8k and HMDI, which becomes more distinct with increasing isocyanate concentration. This region additionally contains combination vibrations of OH groups from residual water [41,42,55], which for pristine PEG 8k appear as a minor band around 5220 cm^{-1} (Fig. 2b). However, these vibrations are not distinguished between the premixes due to their overall low moisture content and minimal variation among the tested samples, as indicated by the Karl Fischer titration study (Table S2).

3.2. *Calculation of the PLS regression for quantitative evaluation of the model premixes*

Generating a PLS model for quantifying unreacted HMDI in a reactive system using spectra from non-reactive material formulations requires that the calibration dataset accurately captures features reflecting the presence of NCO species. While the primary chemical information represented by changes in the NCO bands is expected to remain consistent between the premixes and a reacting material, the remaining spectral regions will vary significantly. As the NCO concentration in the non-reactive premixes is controlled by the monomer ratio in the formulation, the spectra also contain features correlating to the content of other functional groups and the cycloaliphatic and aliphatic monomer chains, as described above. In contrast, when the monomers initially present in a reactive system undergo polymerisation, neither the content nor the structure of the monomer backbones changes, whereas the depletion of NCO species leads to the formation of new chemical structures — urethane, urea, or allophanate linkages — which are correspondingly embedded in the spectra. Including those regions in the model would introduce variability unrelated to unreacted HMDI, distorting quantification and undermining the typical advantages of using

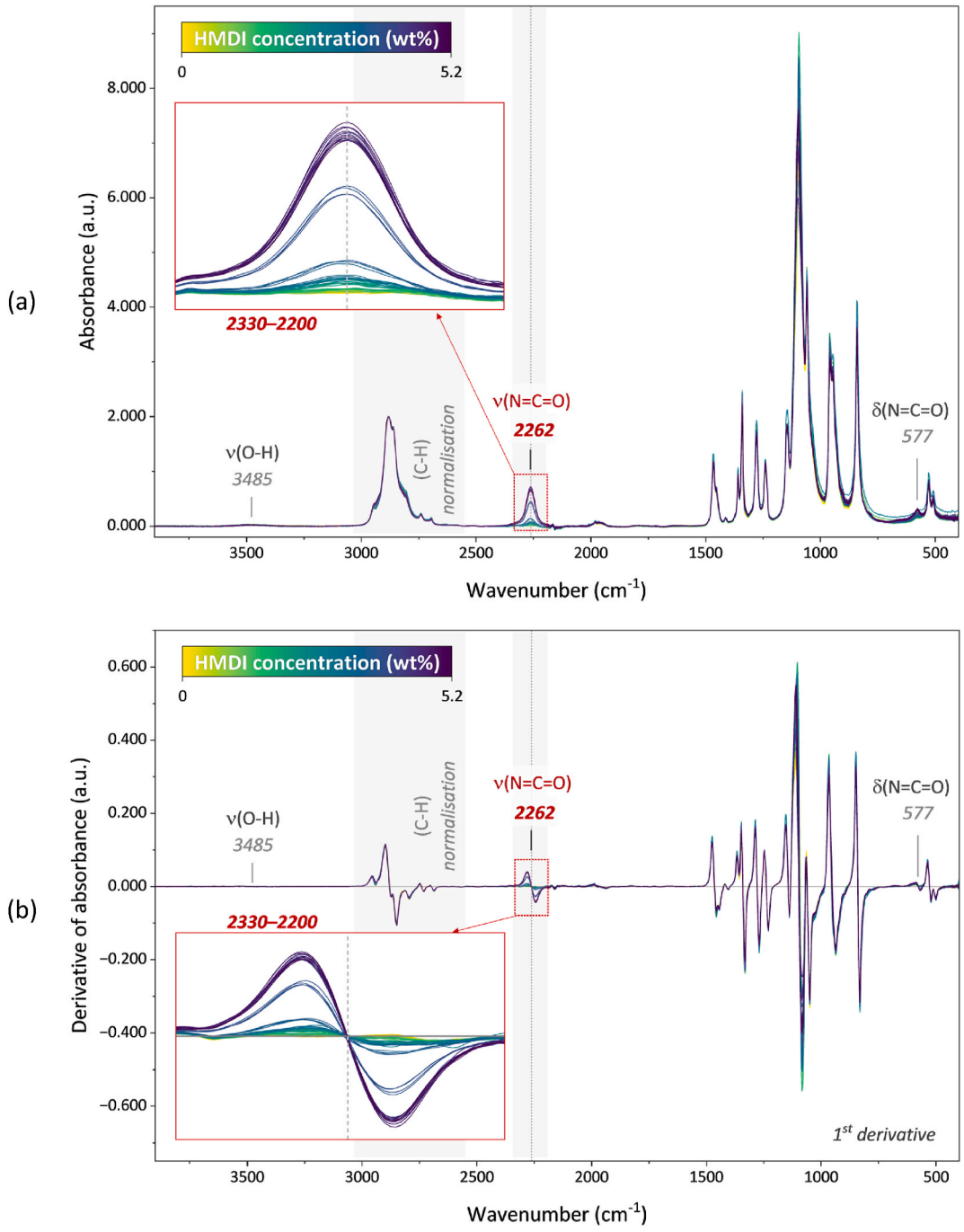

Fig. 3. Pretreated MIR spectra of model premixes with PEG 8k and HMDI at varied concentrations, showing a zoom on the wavenumber range used for calculations of the MIR PLS model (*ν*: stretching modes, δ: bending modes): (a) Normalized; (b) First-order derivative.

broad spectral windows, such as improved robustness to stochastic noise. Therefore, in the performed calibration, only spectral intervals characteristic of the NCO group were selected for the predictor dataset, aligning with the intended use of the model for monitoring reaction progress in PU synthesis.

The normalized MIR spectra showed that the concentration of HMDI in the model premixes strongly correlates with the absorbance of the NCO groups at around 2260 cm^{-1}, which is separated from other characteristic vibrations and unaffected by any phenomena apart from the presence of NCO species. Therefore, the spectral region in the proximity of this band is a suitable marker for their quantification in the non-reactive premix formulations and can be applied in the evaluation of reactive material systems. Before calculation of the MIR PLS model, the baseline drift and offset remaining after the normalization were resolved by first-order derivative using a Savitzky-Golay filter. The bipolar absorbance function obtained from the derivative spectra (Fig. 3b) indicated the wavenumber range between 2330 and 2200 cm^{-1} relevant for the quantitative evaluation of the selected NCO band. Accordingly, this area was used as the predictor dataset for the PLS regression, with the known HMDI concentration in the corresponding premixes assigned as the response variable. The MIR PLS model was generated applying Simplified PLS algorithm based on fully pretreated and mean-centred data from 60 MIR spectra and validated through the contiguous block cross-validation method suitable for sequential datasets.

The resulting MIR calibration model used one PLS factor (latent variable, Fig. 5a) and explained 99.56 % of the variance in the HMDI

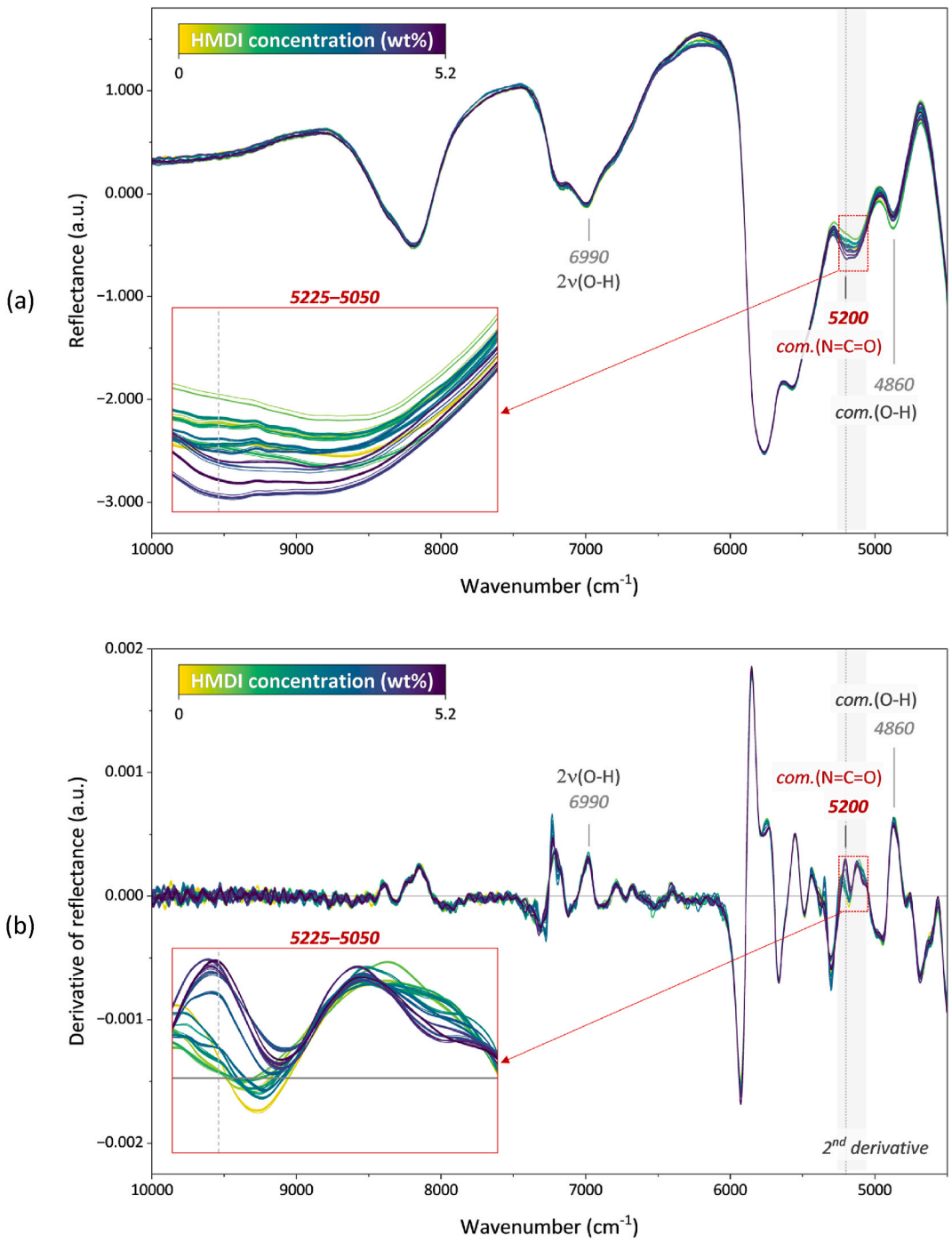

Fig. 4. Pretreated NIR spectra of model premixes with PEG 8k and HMDI at varied concentrations, showing a zoom on the wavenumber range used for calculations of the NIR PLS model (*ν*: stretching modes, com.: combination vibrations): (a) Normalized and smoothed; (b) Second-order derivative.

concentration. It showed a strong linear correlation between the experimental HMDI content in the premixes and the values predicted by the PLS model, as indicated by the regression plots of the experimental data against the values calculated during calibration and cross-validation (Fig. 6a and b). Both the calibration and validation steps yielded a high coefficient of determination (calibration $R^2 \approx 0.996$) reflecting good accuracy. The root mean square error of cross-validation (RMSECV) of 0.152 wt% further indicates strong predictive performance, while its relatively small increase compared to the root mean square error of calibration (RMSEC) suggests that the model retains reasonable robustness within the evaluated dataset. Moreover, the regression plot reveals subtle patterns: the fit is tight at lower HMDI concentrations, with slightly larger deviations at higher concentrations. This trend may result from the inherent immiscibility between HMDI and PEG 8k, leading to phase separation in the unagitated premixes, which accelerates with increasing content of HMDI as the lower fraction component [17]. These observations suggest that the MIR model effectively captures the overall underlying relationship, while also revealing limitations of the off-line setting of the measuring technique.

Since the NIR region exhibits closely spaced as well as overlapping bands around the NCO absorption at 5200 cm^{-1}, selecting a suitable wavelength for quantifying HMDI relied on subtle indicators and appropriate pretreatment of the derivative spectra. Consequently, the wavelength range of 5225–5050 cm^{-1} was chosen for the NIR PLS

Table 1
Absorption bands of characteristic groups in PEG 8k and HMDI detected in the NIR region between 10000 and 4500 cm^{-1} and in the MIR region between 3900 and 400 cm^{-1}.

Wavenumber (cm^{-1})	Component	Group	Vibration
6990	PEG 8k	O-H	Stretching (1st overtone) [32,52]
5200	HMDI	N=C=O	Combination [53]
4860	PEG 8k	O–H	Combination [32,52]
3680	HMDI	N=C=O	Stretching (1st overtone) [46]
3485	PEG 8k	O–H	Stretching [43,44]
2260	HMDI	N=C=O	Stretching [42,45]
1762	HMDI	C=O (uretdione)	Stretching [47–50]
1096	PEG 8k	C–O	Stretching [43,44]
577	HMDI	N=C=O	Bending [42,45]

regression and its response to the information carried by the predictor dataset was further evaluated based on the obtained performance metrics. The model was developed using data from 130 pretreated NIR spectra, following the computation approach as used for the MIR dataset.

The NIR model was calculated using two factors, with the first accounting for 99.29 % and the second contributing 0.46 % of the total variance, resulting in a calibration R^2 of 0.997. Since the variance explained by the first factor is sufficiently high for the quantification approach, the second factor could be discarded to simplify the model and improve its stability. However, the distinctive peaks and noise-free profiles visible in the NIR loading plots (Fig. 5b) indicate that the second NIR factor may represent valuable information about the system and should be included for application testing. This is supported by the strong performance metrics of the NIR model in both calibration and cross-validation (Table 2), which additionally showed a minor improvement over the MIR model, including a lower RMSECV of 0.138 wt%, suggesting enhanced generalizability.

While the NIR model demonstrates effective behaviour during training under a consistently controlled conditions, certain spectral variations could influence its predictions on new datasets. Such variations may arise, for example, due to the capture of additional information related to excessive moisture content in the cases of reactant contamination, since the wavenumber range used for PLS regression overlaps with vibrational frequencies from water [41]. Nevertheless, the achieved performance suggests that the NIR model responds adequately to the composition of the HMDI and PEG 8k mixtures, and its predictive ability remains unaffected as long as the maintained range of water content (Table S3) meets the standard purity criteria required for PU reagents. These characteristics could be reflected in the NIR regression plots (Fig. 6c and d), which, in contrast to the MIR model (Fig. 6a and b), present a consistent fit with a minimal scatter, regardless of the HMDI concentration. It could also indicate that the previously mentioned phase segregation effect, suspected to have a minor impact on the calibration MIR data, is mitigated by continuous homogenisation at elevated temperature in the on-line NIR measurement setting, possibly contributing to the slightly better performance metrics of the NIR model compared to the MIR model (Table 2). Therefore, the latter observation is relevant when collecting calibration spectra that accurately correlate with the NCO content modulated in non-reactive premixes, while it is expected to become negligible in polymerising systems with enhanced phase mixing.

It should be further considered that the factors influencing the performance of MIR and NIR quantification protocols in monitoring PU

Table 2
Parameters of the MIR and NIR PLS models for quantifying isocyanate content in the studied material system, developed using spectral data from non-reactive premixes of PEG 8k and HMDI at varied concentrations.

Model	Calibration				Cross-Validation			
	Slope	Intercept	R^2	RMSEC (wt%)	Slope	Intercept	R^2	RMSECV (wt%)
MIR 1-factor	0.996	0.00686	0.996	0.132	0.994	0.00854	0.994	0.152
NIR 2-factor	0.998	0.00487	0.997	0.106	0.991	0.01306	0.996	0.138

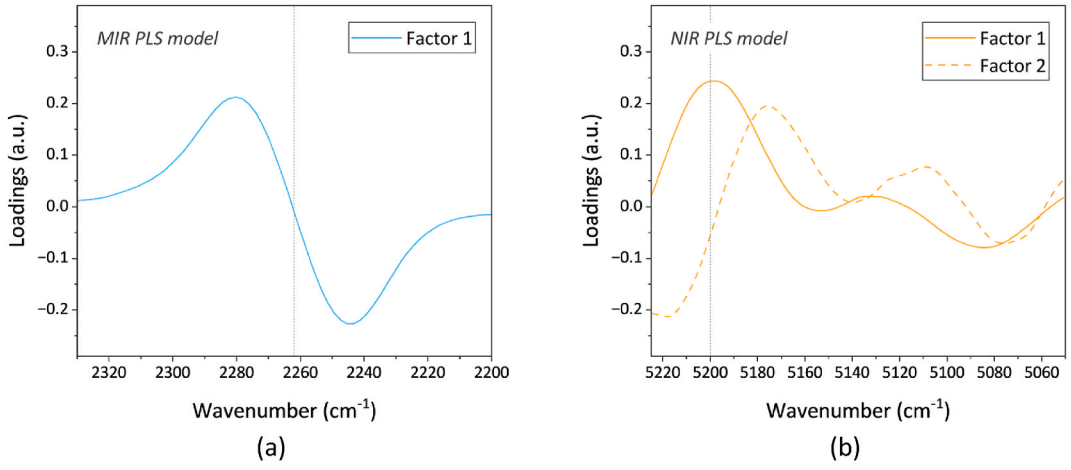

Fig. 5. Loading plots of PLS multivariate regression models: (a) One-factor MIR PLS model with an explained variance of 99.56 %; (b) Two-factor NIR PLS model with a total explained variance of 99.75 % (first factor: 99.29 %, second factor: 0.46 %).

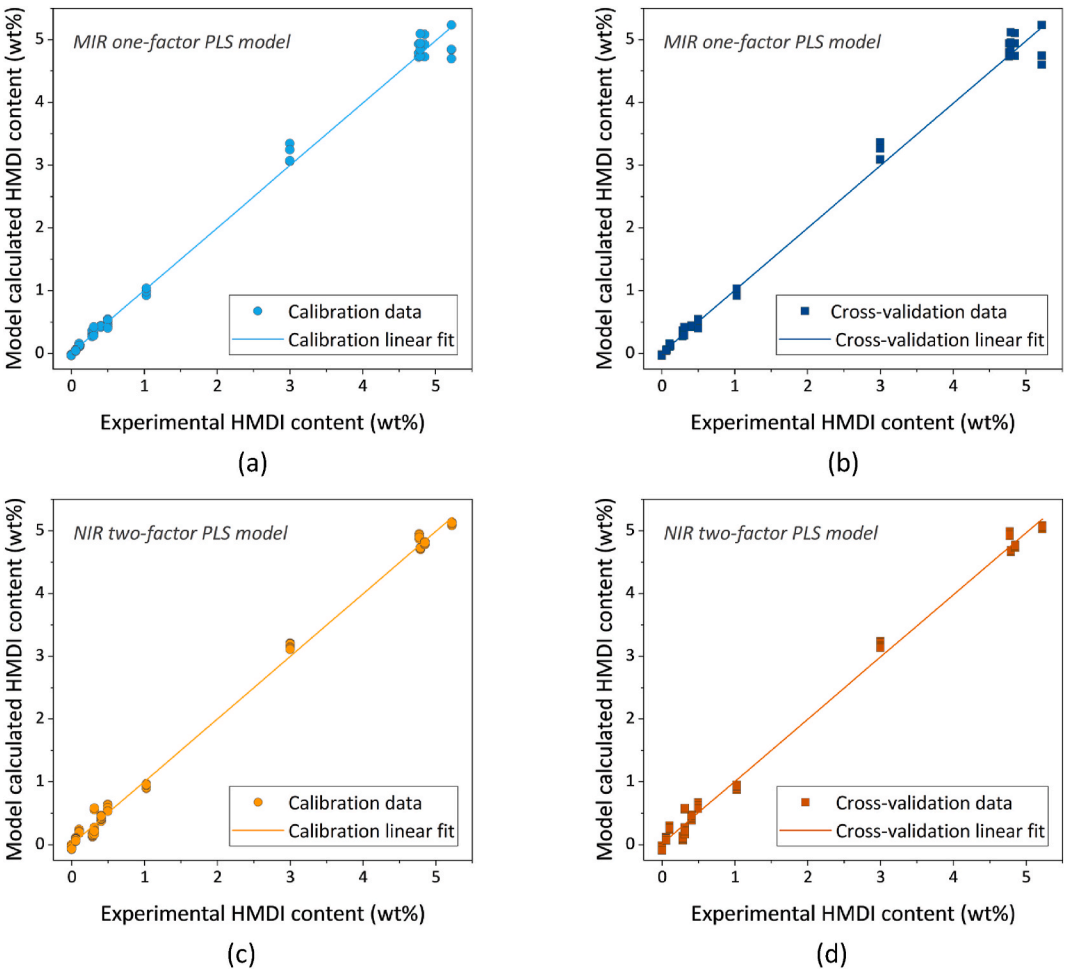

Fig. 6. Regression plots showing the correlation between the experimental content of HMDI in the model premixes and the predicted values, calculated during the modelling step: (a) MIR model calibration; (b) MIR model cross-validation; (c) NIR model calibration; (d) NIR model cross-validation.

reactions will differ due to the intrinsic characteristics of the two spectroscopic techniques. As previously noted, building a PLS model based on non-reactive formulations requires that the calibration data be sufficiently representative of spectral changes occurring in the reactive system. For off-line MIR characterisation, where spectra primarily reflect chemical composition, such a model can typically be applied as a drop-in solution, assuming an appropriate sampling procedure. In contrast, alongside chemical information, NIR spectra also capture physical phenomena related to material properties and the measurement environment, which must remain consistent between calibration and

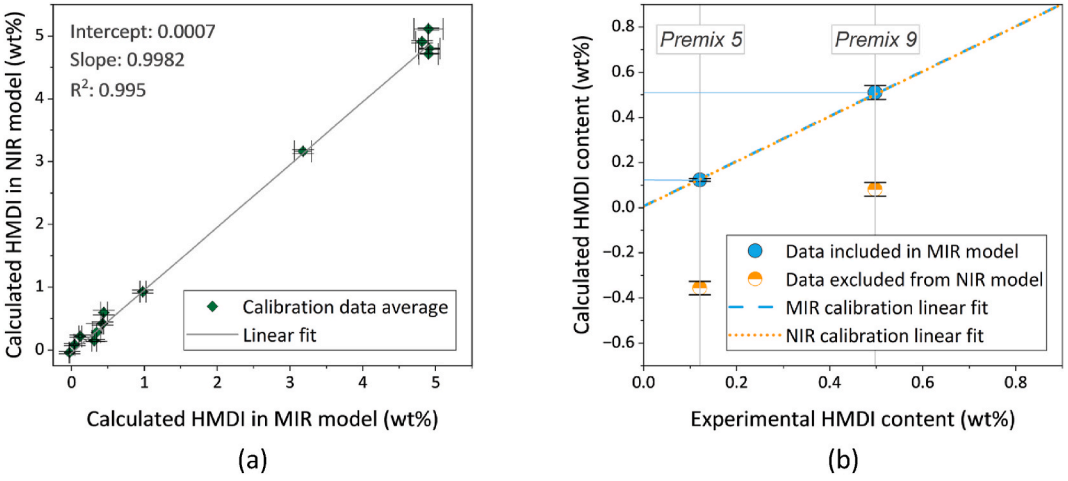

Fig. 7. Comparison of MIR and NIR model predictions for HMDI content in the premix formulations: (a) Regression plot showing the correlation between predicted values by both models across the calibration dataset (R^2: 0.995, slope: 0.9982, intercept: 0.0007); (b) Predicted versus experimental HMDI content for samples included in the MIR calibration model but excluded from the NIR model due to deviations in prediction, linked to anomalies in the NIR spectra.

application of the quantification protocol. While this is addressed by conducting the on-line calibration measurements in a temperature-controlled capillary bypass — a setup that is technically reproducible in a REX line and reflects initial temperature- and viscosity-related scattering — it does not account for the spectral dynamics introduced by progressing conversion or variable processing conditions. To assess whether processing-related factors could alter the spectral response and potentially affect the predictive accuracy of the NIR model, targeted verification under relevant conditions is necessary. For this purpose, the established combination of on-line NIR and at-line MIR models — which showed strong agreement in their predicted values during calibration, as illustrated in Fig. 7a — offers an efficient means of confirming robustness and applicability for further use.

This principle could be similarly applied during implementation as in the calibration stage, where combining both techniques allowed identification of singular measurements showing discrepancies in the HMDI content predicted by the MIR and NIR models for the same premix formulations (Table S2). As shown in Fig. 7b, the MIR model predictions for the affected premixes aligned well with the experimentally added HMDI concentrations, while the corresponding NIR predictions deviated substantially, which justified their exclusion from the NIR calibration dataset. Although the NIR spectra exhibited subtle features distinct from those of other specimens in the same concentration range (Fig. S20—22), they could not be identified as anomalies based solely on the spectral pattern, due to the less distinctive nature of the NIR region. These deviations are suspected to originate either from contamination or from technical artefacts. In contrast, the MIR spectra collected from extruded material after the on-line NIR characterization were consistent with those obtained directly from the premixed batches for the affected premixes (Figure S6, 8 and 12) and other specimens in that range (Figure S5, 7 and 13), confirming their correct inclusion in the MIR calibration dataset. In this context, the combined use of on-line NIR and at-line MIR spectroscopy offers a practical and efficient framework for verification: first to validate the performance of the NIR model, and subsequently to ensure the long-term reliability of in-situ NIR monitoring under production-relevant conditions [18].

4. Conclusions

Our study demonstrates that PLS calibration models for estimating the content of isocyanate species in PU monomer systems can be successfully developed using both at-line MIR and on-line NIR spectroscopic data, bypassing the need to first establish a reaction protocol. Instead, we obtained the necessary spectral data from non-reactive mixtures of polyol and diisocyanate, using an exemplary set of high-molar-mass PEG 8k and HMDI suited for synthesis of HEUR as water-soluble PU-based rheological additives. In practice, this methodology can be extended to a variety of material formulations, for which it is possible to accurately capture the spectral features of the reagents integral to changes in conversion.

A key prerequisite of our protocol was to produce robust calibration models using only a moderate amount of data from a relatively simple series of experiments. This was achieved by ensuring the representativeness of the data and applying appropriate spectral pretreatments. First, the preprocessing of the raw spectra was carefully tailored to each spectroscopic technique, which allowed us to isolate the wavenumber ranges carrying the essential chemical information with minimal interference from extraneous factors. This also maximized signal stability and mitigated the impact of experimental and instrumental noise. Second, we rigorously assessed how well the PLS models fit the calibration data and confirmed that the dataset was self-consistent and homogeneous — something not readily feasible with simpler, univariate methods. We estimated the generalization error of the PLS models directly via cross-validation, using the full dataset in rotation rather than setting aside a portion of data for separate testing. Since both the NIR and MIR models explained over 99.5 % of the variance in HMDI concentration and achieved RMSECV values below 0.16 wt%, their performance falls within the expected range for effective spectroscopic quantification tools [13,21,23,52].

Both models showed a good fit across the entire studied concentration range, underscoring their potential to track the conversion of the isocyanate component throughout the course of HEUR synthesis, used here as an exemplary PU system. Moreover, because the MIR and NIR calibration results were strongly correlated, combining the two techniques as cross-references offers a pathway to further refine these monitoring protocols in real REX applications. This is particularly important for evaluating how well NIR can monitor a reactive manufacturing process, where additional factors come into play, i.a. changes in viscosity and temperature, which cannot be exhaustively investigated during calibration. If such factors influence the NIR spectra of an actual REX process [18,32], at-line MIR measurements can be used to verify and, if necessary, recalibrate the NIR model under the new conditions. Together, this combined approach can expedite the establishment of real-time NIR monitoring — one of the most practical and robust tools for in-process analysis — and facilitate its long-term maintenance by periodically verifying it against MIR. Therefore, with this study we have reached the first stage in developing spectroscopic quantification protocols, which, in subsequent work, will be integrated into a newly engineered REX process for the synthesis of specialty PUs, paving the way for implementing these monitoring tools at an industrial production scale.

CRediT authorship contribution statement

Aleksandra M. Fage: Writing – review & editing, Writing – original draft, Visualization, Project administration, Methodology, Investigation, Funding acquisition, Data curation, Conceptualization, Formal analysis. **Christian A. Backhaus:** Writing – review & editing, Writing – original draft, Visualization, Methodology, Investigation, Formal analysis, Data curation. **Wolfgang Becker:** Writing – review & editing, Writing – original draft, Methodology, Formal analysis. **Günter Lorenz:** Supervision, Conceptualization. **Anita Lorenz:** Writing – review & editing, Methodology. **Karsten Rebner:** Writing – review & editing, Formal analysis. **Frank Henning:** Writing – review & editing.

Declaration of generative AI and AI-assisted technologies in the writing process

During the preparation of this work, the authors used ChatGPT Pro (OpenAI) to improve the readability and language of the manuscript. After using this tool, the authors reviewed and edited the content as needed and take full responsibility for the content of the published article.

Declaration of competing interest

The authors declare that they have no known competing financial interests or personal relationships that could have appeared to influence the work reported in this paper.

Acknowledgments

The research has received funding from the European Union's Horizon research and innovation programs under Grant Agreement No. 820716 (project SIMPLIFY) and No. 101058279 (project SIMPLI-DEMO). The authors gratefully acknowledge Clariant AG for the generous provision of poly(ethylene glycol) Polyglykol 8000 S, as well as Covestro AG and CSC JÄKLECHEMIE GmbH for the donation of dicyclohexylmethane-4,4′-diisocyanate Desmodur® W, which were integral to this study. Furthermore, Christof Hübner, Carolyn Fisher, Robin Töller, Kerstin Sachsenheimer, Matthias Stricker, Wenka Schweikert and Stefan Müller are kindly acknowledged for their

valuable insights and experimental support during the preparation of this work.

Appendix A. Supplementary data

Supplementary data to this article can be found online at https://doi.org/10.1016/j.polymertesting.2025.108925.

Data availability

Data will be made available on request.

References

[1] C. Tzoganakis, Reactive extrusion of polymers: a review, Adv. Polym. Technol. 9 (1989) 321–330, https://doi.org/10.1002/adv.1989.060090406.

[2] D. Wołosz, A.M. Fage, P.G. Parzuchowski, A. Świderska, R. Brüll, Reactive extrusion synthesis of biobased isocyanate-free hydrophobically modified ethoxylated urethanes with pendant hydrophobic groups, ACS Sustain. Chem. Eng. 10 (2022) 11627–11640, https://doi.org/10.1021/acssuschemeng.2c03535.

[3] J.-M. Raquez, R. Narayan, P. Dubois, Recent advances in reactive extrusion processing of biodegradable polymer-based compositions, Macromol. Mater. Eng. 293 (2008) 447–470, https://doi.org/10.1002/mame.200700395.

[4] S. Ash, R. Sharma, M. Naveed, S. Patil, S. Cheng, M. Rabnawaz, A continuous melt extrusion approach toward polyethylene-based vitrimers with improved crosslinking and performance, J. Appl. Polym. Sci. 141 (2024) e55652, https://doi.org/10.1002/app.55652.

[5] A. Datta Sarma, S.V. Zubkevich, F. Addiego, D.F. Schmidt, A.S. Shaplov, V. Berthé, Synthesis of High- Tg nonisocyanate polyurethanes via reactive extrusion and their batch foaming, Macromolecules 57 (2024) 3423–3437, https://doi.org/10.1021/acs.macromol.4c00222.

[6] Y. Zhuang, N. Saadatkhah, M.S. Morgani, T. Xu, C. Martin, G.S. Patience, A. Ajji, Experimental methods in chemical engineering: reactive extrusion, Can. J. Chem. Eng. 101 (2023) 59–77, https://doi.org/10.1002/cjce.24538.

[7] E. Delebecq, J.-P. Pascault, B. Boutevin, F. Ganachaud, On the versatility of urethane/urea bonds: reversibility, blocked isocyanate, and non-isocyanate polyurethane, Chem. Rev. 113 (2013) 80–118, https://doi.org/10.1021/cr300195n.

[8] J.P. Reynolds, J.R. Brown, A. Das, T.E. Long, P. Willoughby, J. Delaney, T. Dyndikova, M.J. Bortner, Characterization methods to predict extrusion performance in thermoplastic polyurethane batches, Polym. Degrad. Stabil. 224 (2024) 110746, https://doi.org/10.1016/j.polymdegradstab.2024.110746.

[9] M. Cegla, A. Fage, S. Kemmerling, S. Engell, Optimal design and operation of reactive extrusion processes: application to the production and scale-up of polyurethane rheology modifiers for paints, Polym. Eng. Sci. 63 (2023) 4220–4235, https://doi.org/10.1002/pen.26519.

[10] J.-P. Puaux, P. Cassagnau, G. Bozga, I. Nagy, Modeling of polyurethane synthesis by reactive extrusion, Chem. Eng. Process. Process Intensif. 45 (2006) 481–487, https://doi.org/10.1016/j.cep.2005.11.006.

[11] J. Zhou, Z. Liu, Z. Zhu, Z. Zeng, L. Sun, The kinetics of the polyurethane moisture curing reaction: a combined experimental and DFT mechanistic study, React. Chem. Eng. 10 (2024) 38–47, https://doi.org/10.1039/D4RE00385C.

[12] A. Bampouli, I. Tzortzi, A. de Schutter, K. Xenou, G. Michaud, G.D. Stefanidis, T. van Gerven, Insight into solventless production of hydrophobically modified ethoxylated urethanes (HEURs): the role of moisture concentration, reaction temperature, and mixing efficiency, ACS Omega 7 (2022) 36567–36578, https://doi.org/10.1021/acsomega.2c04530.

[13] P.D. Coates, S.E. Barnes, M.G. Sibley, E.C. Brown, H. Edwards, I.J. Scowen, In-process vibrational spectroscopy and ultrasound measurements in polymer melt extrusion, Polymer 44 (2003) 5937–5949, https://doi.org/10.1016/S0032-3861(03)00544-5.

[14] C. Abeykoon, Sensing technologies for process monitoring in polymer extrusion: a comprehensive review on past, present and future aspects, measurement, Sensors 22 (2022) 100381, https://doi.org/10.1016/j.measen.2022.100381.

[15] S. Parnell, K. Min, M. Cakmak, Kinetic studies of polyurethane polymerization with Raman spectroscopy, Polymer 44 (2003) 5137–5144, https://doi.org/10.1016/S0032-3861(03)00468-3.

[16] S. Benali, J. Bouchet, G. Lachenal, Chemeorheology: a new design for simultaneous rheological and fourier transform near infrared analysis, J. Near Infrared Spectrosc. 12 (2004) 5–13, https://doi.org/10.1255/jnirs.403.

[17] V.W.A. Verhoeven, M.P.Y. van Vondel, K.J. Ganzeveld, L.P.B.M. Janssen, Rheo-kinetic measurement of thermoplastic polyurethane polymerization in a measurement kneader, Polym. Eng. Sci. 44 (2004) 1648–1655, https://doi.org/10.1002/pen.20163.

[18] P. Hitzer, T. Bäuerle, T. Drieschner, E. Ostertag, K. Paulsen, H. van Lishaut, G. Lorenz, K. Rebner, Process analytical techniques for hot-melt extrusion and their application to amorphous solid dispersions, Anal. Bioanal. Chem. 409 (2017) 4321–4333, https://doi.org/10.1007/s00216-017-0292-z.

[19] Y. Wang, B. Steinhoff, C. Brinkmann, I. Alig, In-line monitoring of the thermal degradation of poly(l-lactic acid) during melt extrusion by UV–vis spectroscopy, Polymer 49 (2008) 1257–1265, https://doi.org/10.1016/j.polymer.2008.01.010.

[20] L.P. Barros, S.V. Canevarolo, D. Klein, J. Maia, On-line ATR-MIR for real-time quantification of chemistry kinetics along the barrel in extrusion-based processes, Polym. Test. 103 (2021) 107350, https://doi.org/10.1016/j.polymertesting.2021.107350.

[21] J.C. Steinbach, M. Schneider, O. Hauler, G. Lorenz, K. Rebner, A. Kandelbauer, A process analytical concept for In-Line FTIR monitoring of polysiloxane formation, Polymers (Basel) 12 (2020), https://doi.org/10.3390/polym12112473.

[22] X. Lopez de Pariza, T. Erdmann, P.L. Arrechea, L. Perez, C. Dausse, N.H. Park, J. L. Hedrick, H. Sardon, Synthesis of tailored segmented polyurethanes utilizing continuous-flow reactors and real-time process monitoring, Chem. Mater. 33 (2021) 7986–7993, https://doi.org/10.1021/acs.chemmater.1c01919.

[23] F.A. DeThomas, J.W. Hall, S.L. Monfre, Real-time monitoring of polyurethane production using near-infrared spectroscopy, Talanta 41 (1994) 425–431, https://doi.org/10.1016/0039-9140(93)E0055-I.

[24] T. Furukawa, Y. Kita, S. Sasao, K. Matsukawa, M. Watari, S. Šašic, H.W. Siesler, Y. Ozaki, On-Line monitoring of melt-extrusion transesterification of ethylene vinylacetate copolymers by near infrared spectroscopy and chemometrics, J. Near Infrared Spectrosc. 10 (2002) 195–202, https://doi.org/10.1255/jnirs.335.

[25] S. Benali, D. Bertrand, J. Dupuy, G. Lachenal, A. Maazouz, In situ monitoring of polyurethane cure using fibre-optical FT-NIR spectroscopy, Trans. Inst. Meas. Control 29 (2007) 417–429, https://doi.org/10.1177/0142331207079812.

[26] L. Moghaddam, D.J. Martin, P.J. Halley, P.M. Fredericks, Vibrational spectroscopic studies of laboratory scale polymer melt processing: application to a thermoplastic polyurethane nanocomposite, Vib. Spectrosc. 51 (2009) 86–92, https://doi.org/10.1016/j.vibspec.2008.10.015.

[27] I. Yoshikawa, Y. Hikima, M. Ohshima, In-Line chemical composition monitoring for the injection molding process of biodegradable polymer blends using simultaneous measurement of near-infrared diffuse reflectance and transmission spectra, Appl. Spectrosc. 78 (2024) 933–941, https://doi.org/10.1177/00037028241247823.

[28] S. Ulitzsch, T. Bäuerle, M. Stefanakis, M. Brecht, T. Chassé, G. Lorenz, A. Kandelbauer, Synthesis of an addition-crosslinkable, silicon-modified polyolefin via reactive extrusion monitored by In-Line raman spectroscopy, Polymers (Basel) 13 (2021), https://doi.org/10.3390/polym13081246.

[29] C.A. Cateto, M.F. Barreiro, A.E. Rodrigues, Monitoring of lignin-based polyurethane synthesis by FTIR-ATR, Ind. Crop. Prod. 27 (2008) 168–174, https://doi.org/10.1016/j.indcrop.2007.07.018.

[30] H. Madra, S.B. Tantekin-Ersolmaz, F.S. Guner, Monitoring of oil-based polyurethane synthesis by FTIR-ATR, Polym. Test. 28 (2009) 773–779, https://doi.org/10.1016/j.polymertesting.2009.05.013.

[31] K.B. Beć, J. Grabska, J. Badzoka, C.W. Huck, Spectra-structure correlations in NIR region of polymers from quantum chemical calculations. The cases of aromatic ring, C=O, C≡N and C-Cl functionalities, Spectrochim. Acta Mol. Biomol. Spectrosc. 262 (2021) 120085, https://doi.org/10.1016/j.saa.2021.120085.

[32] L.G. Weyer, S.-C. Lo (Eds.), Handbook of Vibrational Spectroscopy: Spectra-Structure Correlations in the Near-Infrared, John Wiley & Sons, Ltd, 2006.

[33] G. Shmueli, S. Ray, J.M. Velasquez Estrada, S.B. Chatla, The elephant in the room: predictive performance of PLS models, J. Bus. Res. 69 (2016) 4552–4564, https://doi.org/10.1016/j.jbusres.2016.03.049.

[34] M. Salzmann, Y. Blößl, A. Todorovic, R. Schledjewski, Usage of near-infrared spectroscopy for inline monitoring the degree of curing in RTM processes, Polymers (Basel) 13 (2021), https://doi.org/10.3390/polym13183145.

[35] K. Hailu, G. Guthausen, W. Becker, A. König, A. Bendfeld, E. Geissler, In-situ characterization of the cure reaction of HTPB and IPDI by simultaneous NMR and IR measurements, Polym. Test. 29 (2010) 513–519, https://doi.org/10.1016/j.polymertesting.2010.03.001.

[36] Thomas Rohe, Wolfgang Becker, Sabine Kölle, Norbert Eisenreich, Peter Eyerer, Near infrared (NIR) spectroscopy for in-line monitoring of polymer extrusion processes, Talanta 50 (1999) 283–290, https://doi.org/10.1016/S0039-9140(99)00035-1.

[37] B. Quienne, J. Pinaud, J.-J. Robin, S. Caillol, From architectures to cutting-edge properties, the blooming world of hydrophobically modified ethoxylated urethanes (HEURs), Macromolecules 53 (2020) 6754–6766, https://doi.org/10.1021/acs.macromol.0c01353.

[38] I. Tzortzi, C. Xiouras, C. Choustoulaki, A. Tzani, A. Detsi, G. Michaud, T. van Gerven, G.D. Stefanidis, One-step versus two-step synthesis of hydrophobically modified ethoxylated urethanes: benefits and limitations, Ind. Eng. Chem. Res. 62 (2023) 11378–11391, https://doi.org/10.1021/acs.iecr.3c01107.

[39] G. Odian, Principles of Polymerization: Step Polymerization, John Wiley & Sons, Ltd, 2004.

[40] M. Szycher, Szycher's Handbook of Polyurethanes, second ed., CRC Press, 2012.

[41] V. Moll, K.B. Beć, J. Grabska, C.W. Huck, Investigation of water interaction with polymer matrices by near-infrared (NIR) spectroscopy, Molecules 27 (2022), https://doi.org/10.3390/molecules27185882.

[42] G. Socrates, Infrared and Raman Characteristic Group Frequencies: Tables and Charts, Thirdrd, John Wiley & Sons, Ltd, 2004.

[43] T. Kumar, Fourier transform infrared spectrometric determination of polyethylene glycol in high-density polyethylene, Analyst 115 (1990) 1597–1599, https://doi.org/10.1039/AN9901501597.

[44] Hiroatsu Matsuura, Tatsuo Miyazawa, Katsunosuke Machida, Infrared spectra of poly(ethylene glycol) dimethyl ethers in the crystalline state, Spectrochim. Acta Mol. Spectros 29 (1973) 771–779, https://doi.org/10.1016/0584-8539(73)80044-3.

[45] P. Alagi, R. Ghorpade, Y.J. Choi, U. Patil, I. Kim, J.H. Baik, S.C. Hong, Carbon dioxide-based polyols as sustainable feedstock of thermoplastic polyurethane for

corrosion-resistant metal coating, ACS Sustainable Chem. Eng. 5 (2017) 3871–3881, https://doi.org/10.1021/acssuschemeng.6b03046.
[46] D.J. David, A study of the near-infrared spectra of some aliphatic and aromatic isocyanates, Anal. Chem. 35 (1963) 37–44, https://doi.org/10.1021/ac60194a012.
[47] H. Bakhshi, S. Agarwal, Dendrons as active clicking tool for generating non-leaching antibacterial materials, Polym. Chem. 7 (2016) 5322–5330, https://doi.org/10.1039/C6PY01105E.
[48] Douglas A. Wicks, Zeno W. Wicks, Blocked isocyanates III: part A. Mechanisms and chemistry, Prog. Org. Coating 36 (1999) 148–172, https://doi.org/10.1016/S0300-9440(99)00042-9.
[49] E. Querat, L. Tighzert, J.P. Pascault, K. Dušek, Blocked isocyanate. Reaction and thermal behaviour of the toluene 2,4-diisocyanate dimer, Angew. Makromol. Chem. 242 (1996) 1–36, https://doi.org/10.1002/apmc.1996.052420101.
[50] S. Harling, G. Meola, S. Schaible, A. Schulthess, C. Braendli, O. Meincke, Latent reactive polyurethanes based on toluenediisocyanate-uretdione and polycaprolactones, Int. J. Adhesion Adhes. 46 (2013) 26–33, https://doi.org/10.1016/j.ijadhadh.2013.05.012.
[51] J.D. Roscioli, M. Desanker, K.A. Patankar, A. Grzesiak, X. Chen, Simultaneous high-throughput monitoring of urethane reactions using near-infrared hyperspectral imaging, Appl. Spectrosc. 76 (2022) 1329–1334, https://doi.org/10.1177/00037028221110914.
[52] R.L. Brashear, D.R. Flanagan, P.E. Luner, J.J. Seyer, M.S. Kemper, Diffuse reflectance near-infrared spectroscopy as a nondestructive analytical technique for polymer implants, J. Pharmaceut. Sci. 88 (1999) 1348–1353, https://doi.org/10.1021/js9804821.
[53] Y. Schellekens, B. van Trimpont, P.-J. Goelen, K. Binnemans, M. Smet, M.-A. Persoons, D. de Vos, Tin-free catalysts for the production of aliphatic thermoplastic polyurethanes, Green Chem. 16 (2014) 4401–4407, https://doi.org/10.1039/C4GC00873A.
[54] M. Kwaśniewicz, M.A. Czarnecki, The effect of chain length on mid-infrared and near-infrared spectra of aliphatic 1-Alcohols, Appl. Spectrosc. 72 (2018) 288–296, https://doi.org/10.1177/0003702817732253.
[55] X. Chen, K.A. Patankar, M. Larive, Monitoring polyurethane foaming reactions using near-infrared hyperspectral imaging, Appl. Spectrosc. 75 (2021) 46–56, https://doi.org/10.1177/0003702820941877.
[56] S. Körber, K. Moser, J. Diemert, Development of high temperature resistant stereocomplex PLA for injection moulding, Polymers 14 (2022) 384, https://doi.org/10.3390/polym14030384.